Molecular mechanism behind the involvement of apple flavonoid glycosyltransferase gene *MdGT1* in the color of apple leaves

Pan Li[1#], Hongjuan Ge[2#], Lei Zhang[3#], Jing Shu[4], Zhuojing Sun[5], Lepu Jiang[3], Chengchao Zheng[3], Huairui Shu[3], Guangli Sha[2*], Lusha Ji[1*], Shizhong Zhang[3*]

[1]School of Pharmacy, Liaocheng University, Liaocheng, Shandong, 250000, P.R. China

[2]Qingdao Agriculture Academy, Qingdao, Shandong, 266100, P.R. China

[3]State Key Laboratory of Crop Biology, College of Life Sciences, Shandong Agricultural University, Tai'an, Shandong, 271018, P.R. China

[4]Shandong Agriculture and Engineering University, Jinan, Shandong, 250100, P.R. China

[5]Science and Technology Development Center of Ministry of Agriculture and Rural Affairs

[#]These authors contributed equally to this work.

[*]Corresponding authors:

Shizhong Zhang: shizhong@sdau.edu.cn; Tel: 86-538-8242364

Lusha Ji: Jilusha@lcu.edu.cn; Tel: 86-635-8239774

Guangli Sha: GuangLisha@126.com; Tel: 86-532-87891009

Running title: *MdGT1* involved in flavonoid metabolism

Summary

Flavonoids are a class of polyphenol compounds that are widespread in plants. They play an important role in plant growth and development. In this study, we found a mutant strain of *M. baccata* with yellow leaves (YL). Transcriptome sequencing revealed that it exhibited significant changes in the flavonoid metabolism pathway, which screening revealed was associated with a glycosyltransferase gene, MD09G1064900 (MdGT1). Analysis of its spatiotemporal expression showed that MdGT1 was mainly expressed in the stem and leaves, it means that MdGT1 may have a functional role in these parts. Real-time PCR and HPLC showed that *MdGT1* was significantly upregulated by anthocyanin and exhibited strong anthocyaninase activity *in vitro*, respectively. An *MdGT1* plant expression vector was constructed and overexpressed in apple fruit callus, resulting in a significant decrease of anthocyanin. Phenotypic observation also revealed that the *MdGT1*-overexpressing lines exhibited worse growth than the wild type after NaCl treatment, while they grew better upon the addition of exogenous anthocyanins. Moreover, real-time PCR and physiological data showed that *MdGT1* is involved in salt stress and closely related to antioxidant pathways. Electrophoretic mobility shift assays (EMSA) and yeast one-hybrid experiments also proved that the transcription factor *MdMYB88* is an upstream regulatory factor of *MdGT1*. The sequencing results revealed an amino acid insertion in an *MdMYB88* HTH domain (between 77-131 amino acids) in the YL mutant strain. In conclusion, we identified a new apple glycosyltransferase gene, *MdGT1*, which may affect the color of apple leaves by glycosylating anthocyanins, and be regulated by the upstream transcription factor *MdMYB88*.

Keywords: apple; *MdGT1*; anthocyanin; antioxidant; *MdMYB88*

Significance statement

The glycosyltransferases and their physiological significance in apple are largely unknown. Here we revealed that the *MdMYB88*-regulated apple glycosyltransferase gene *MdGT1* plays a crucial role in the color of apple leaves and enhances plant tolerance to salt by antioxidant pathways via anthocyanin metabolism.

Introduction

Apple is one of the world's most widely cultivated fruits. In traditional Chinese medicine, *M. hupehensis* is used for treating inflammatory diseases because it contains flavonoid glycosides, phenols, and amino acids (Vanderzande et al., 2019). It is a tree with a very rich green color because of its rich

canopy, long life, and beautiful leaf color (Burgess et al., 2017). These features make this species a useful option for landscaping purposes and reforestation.

Flavonoids are polyphenol compounds that are widespread in various plants, and including numerous different types (Matus et al., 2016). To date, more than 7000 flavonoids have been identified in nature, mainly including flavonols, flavones, isoflavones, and anthocyanins (Yonekura-Sakakibara et al., 2008). Flavonoids are mainly synthesized through the propane metabolic pathway. First, chalcone synthase (CHS) catalyzes 4-coumarin-CoA and malonyl CoA to produce chalcone, and then chalcone goes through a series of enzymatic reactions to produce dihydroflavonols (including dihydrokaempferol and dihydroquercetin). Then, dihydroflavonols are produced under the action of flavonoid synthase (FLS) to produce quercetin and kaempferol. Anthocyanins are produced under the action of hydroflavonoid reductase (DFR) (Yonekura-Sakakibara et al., 2014). Finally, the active quercetin, kaempferol, and anthocyanins are modified by various sugar groups in the plant and transported to other parts of the plant in the form of inactive glycosides or stored for later use (Harborne et al., 2000; Winkel-Shirley, 2001).

Many different flavonoids have been identified, many of which share the same metabolic pathway. This makes the metabolic regulation of flavonoids very complicated, with a variety of regulatory factors being involved (Cassidy et al., 2017). Intensive study of the transcriptional regulation of flavonoid metabolism in *Arabidopsis thaliana* has been performed. Three main transcription factors have been identified, namely, MYB transcription factor, bHLH transcription factor, and WD40 protein (Zhao et al., 2019). These transcription factors can bind to the promoters of structural genes involved in flavonoid metabolism to regulate their expression. Similar regulatory mechanisms have also been found in plants such as petunia, corn, apple, and rice. It was also shown that the transcription factor *MdMYB88*/*MdMYB124* act as direct regulators of the *COLD SHOCK DOMAIN PROTEIN 3* (*MdCSP3*) and *CIRCADIAN CLOCK ASSOCIATED 1* (*MdCCA1*) genes involved in cold stress by promoting anthocyanin accumulation and H_2O_2 detoxification (Xie et al., 2018).

Flavonoids, secondary metabolites, play an important role in the growth and development of plants, for example, by participating in plant color formation. As early as 1987, Meyer et al. introduced the DFR gene of maize into morning glory, which resulted in the appearance of a new flower color (Meyer et al., 1987). In recent years, research has shown that the transcription factor *FaMYB10* can affect the color of octoploid strawberries by changing the flavonoid metabolite pathway (Wang et al.,

2018). Moreover, flavonoids have been shown to be involved in plant abiotic stress by eliminating the residual reactive oxygen species (ROS) in plant cells. Active oxygen can cause tremendous damage to the normal development of plants. Therefore, antioxidants that can remove active oxygen have evolved in plants, including superoxide dismutase (SOD), catalase (CAT), ascorbic acid (ascorbate), glutathione (glutathione), peroxidase (peroxidase, POD), and glutathione reductase (Pospisil et al., 2012).

Glycosyltransferases have the ability to transfer sugar groups to small-molecule substances in plants, such as plant hormones, polypeptides, proteins, and secondary metabolites. During the course of glycosyl transfer, the properties of receptor molecules can change, which in turn affects the growth and environmental responses of plants (Tawfeek et al., 2019). Glycosylation can also participate in the responses of plants to abiotic stresses. For example, an *Arabidopsis thaliana* line overexpressing glycosyltransferase *UGT76C2* showed a drought-sensitive phenotype in the seedling stage, but a drought-resistant one at later stages (Li et al., 2015). In addition, studies have shown that glycosylation can participate in plant secondary metabolism. An example of this involved lignin, an important component of plant cell wall synthesis. Without lignin, plant cell walls cannot be synthesized normally, and plants cannot carry out their normal activities. Through *in vitro* enzymatic reactions and studies of plant mutants, Lin et al. proved that the glycosyltransferase *UGT72B1* can glycosylate important precursors of the lignin synthesis pathway, and that strains with mutation of this glycotransferase show lignin accumulation, cell wall thickening, and reduced fertility (Lin et al., 2016). Although great progress has been made in research on the function of plant glycosyltransferases in recent years, studies are predominantly still focused on the model plant *A. thaliana*.

However, some scientists have recently begun to turn their attention to the study of secondary metabolism in apple. For example, in 2010, Velasco et al. sequenced the domesticated apple (*Malus×domestica Borkh*.) genome, which laid the foundation for future research on the functions of apple genes (Velasco et al., 2010). However, owing to the long growth cycle of apples, their complex metabolism, and the associated difficulty in gene cloning, little research of this kind has yet been performed, with even fewer studies having been carried out on genes related to the flavonoid metabolism pathway and flavone glycosyltransferase in apples. However, in 2016, Yahyaa et al. identified a phloretin-4'-O-glycosyltransferase gene (*MdPh-4'-OGT*) from apples (Yahyaa et al., 2016), while the following year Dare et al. silenced a phloretin-specific glycosyltransferase in apples, which disrupted phenylpropane biosynthesis and plant development (Dare et al., 2017). Moreover, Zhou et al.

performed a genome-wide analysis to identify the glycosyltransferase that converts phloretin to phloridzin in apples (Zhou et al., 2017). Furthermore, Elejalde-Palmett et al. conducted a genome-wide identification and biochemical analysis of the *UGT88F* subfamily in apples (Elejalde-Palmett et al., 2019).

In this study, we associated with a glycosyltransferase gene *MdGT1* through transcriptome sequencing. *In vitro* enzymatic experiments and *in vivo* transgenic apple callus experiments revealed the involvement of *MdGT1* in the metabolism of flavonoids and its potential association with the formation of leaf color in apple. This work lays a foundation for the future selection and acquisition of apple germplasm resources.

Results

The observation of biological characteristics

Under normal condition, the leaves and branches of the *M. baccata* are green, but we found a mutant strain during the cultivation process, its leaves were yellow and its stem was red. The new leaves of yellow leaves (YL) were golden and its stem was red, while the new leaves of green leaves (GL) were dark green and its stem was light green (Figure 1a and 1c). Upon the measurement of phenotypic data, the petiole length, leaf width, leaf length, thick petiole, thick stem, and internode length were found to differ significantly between YL and GL strains (Figure 1b). The levels of chlorophyll a, b, carotenoid, and anthocyanin in GL were also significantly higher than those in YL (Figure 1e), and this may be why the leaves are yellow. Furthermore, the main veins of leaves of YL were thinner than those of GL, and their degree of lignification was low (Figure 1d). Western blot results also showed that the chloroplast protein subunits RbcL of GL were significantly redundant with the YL (Figure 1f). The YL phenotypes of these natural variations can indicate that YL growth is poorly and photosynthetic metabolism is affected.

Transcriptome sequencing and determination of the candidate gene *MdGT1*

Two cDNA libraries were constructed from the total RNA of the GL and YL. The numbers of up- and down-regulated unigenes are shown in Figure 2a. To identify the biological pathways activated in *M. hupehensis* leaves, we mapped the annotated sequences to the canonical reference pathways in the Kyoto Encyclopedia of Genes and Genomes (KEGG) database (Figure 2b). From these pathways, we concentrated on the “Biosynthesis of other secondary metabolites” category in relation to leaf pigmentation, and 80 unigenes encoding 14 enzymes were assigned to the flavonoid biosynthetic

pathway based on KEGG pathway assignment. To further analyze the differences between the YL during ripening, five unigenes related to flavonoid biosynthetic pathway (Figure 2c) and five apple glycosyltransferase genes were chosen for qRT-PCR analysis. The results were consistent with those obtained from the DGE expression profiling (Figure 2d, 2e). According to the results, *MdGT1* is the most up-regulated gene. Therefore, we speculate that the mutant strain of *M. baccata* with yellow leaves (YL) may be related to MdGT1. The screening identified the candidate gene *Md09G1064900* (MdGT1) (see Tables S3 and S4 for details).

***MdGT1 in vitro* enzyme activity analysis**

In this study, a phylogenetic tree of all glycosyltransferase genes was constructed using bioinformatics combined with phylogenetic tree construction software (Mega7.0) (Figure 3a). All transferases were found to contain a conserved sequence of 44 amino acids (see the box in Table S2 for details) and had high homology (Figures 3b, S1a). The physical and chemical properties of the glycosyltransferase family are shown in Figure S1b. The results showed that the products encoded by most glycosyltransferase genes are located on the cell membrane.

Real-time PCR analysis of the expression of all glycosyltransferase genes in different anatomical regions of the plant was performed (Figure S2b). *MdGT1* was mainly expressed in the stem and leaf (Figure 3c), which suggests that it may play certain functional roles there.

Transcriptome sequencing results showed that the significant differences between YL and GL in flavonoid synthesis pathways. Therefore, we used flavonoids quercetin, kaempferol and anthocyanins to induce *M. baccata* seedlings. The results showed that the gene *MdGT1* is upregulated by quercetin, kaempferol, and anthocyanins (most significant), which indicates that it may be related to the anthocyanin metabolism pathway (Figure 3e). As anthocyanin metabolism is often closely related to adverse stresses, we determined the expression level of *MdGT1* under various abiotic stresses. Using the results of real-time PCR analysis of the abiotic stress-induced expression of all glycosyltransferase genes, a heat map was constructed, the results of which are shown in Figure S3. As shown in Figure 3d, the gene *MdGT1* was upregulated by NaCl (most significant), ABA, mannitol, and a temperature of 4℃. This indicates that *MdGT1* may be particularly related to salt stress.

Glycosyltransferases are a class of enzymes that can transfer glycosyl groups to other small-molecule compounds. As shown in Figure 3f–3h and Figure S4, *MdGT1* can glycosylate

anthocyanins, quercetin, and kaempferol, but not other compounds of the phenylpropane family *in vitro*. The specific enzyme activity of *MdGT1* to anthocyanin is about 3.47 nkat·mg^{-1}, which is higher than the specific enzyme activities of quercetin and kaempferol. This indicated that the glycosyltransferase *MdGT1* is probably involved in the anthocyanin metabolism pathway.

MdGT1 overexpressed in apple callus promotes anthocyanin accumulation

To further confirm the function of the glycosyltransferase gene *MdGT1* in anthocyanin-related coloring, *MdGT1* was overexpressed in apple fruit callus. *OE4*, *OE9*, and *OE15* lines were used for subsequent experimental studies (Figure 4a). The above research showed that *MdGT1* is significantly induced by salt stress. To further confirm the relationship between *MdGT1* involved in the anthocyanin metabolism pathway and the salt stress pathway, apple fruit calluses were cultivated on salt and anthocyanin medium. As shown in Figure 4b and 4c, on the normal medium, the growth status of callus showed no difference among the lines and the control. However, on the medium containing NaCl, the growth of *OE4*, *OE9*, and *OE15* was significantly worse than that of non-transgenic callus. After the addition of a low level of anthocyanin to the medium, the growth of each callus showed a clear improvement. The anthocyanin was analyzed by HPLC; the results were consistent with the observed phenotype, with higher anthocyanin content being present in the callus exhibiting good growth (Figure 4d). These results indicate that the accumulation of anthocyanins can improve the salt resistance of apple callus.

Flavonoids are natural antioxidants in plants and can remove active oxygen. Under normal conditions, the active oxygen level in the callus is low, but after the treatment with 100 mM NaCl in this study, the active oxygen level increased, while after adding anthocyanin to the medium, the active oxygen level in the callus decreased (Figure 4e). These results show that the increase in salt resistance of callus is due to the scavenging of active oxygen by anthocyanins. The total antioxidant capacity in each callus was also measured; contrary to the results regarding the level of active oxygen, the total antioxidant capacity in the calluses overexpressing *OE4*, *OE9*, and *OE15* showed a significant decrease (Figure 4f). The levels of glutathione and ascorbic acid in each callus were also determined, with the results shown in Figure 4g and 4h. There was basically no difference in the levels of glutathione and ascorbic acid in each callus among the different lines. These results indicated that *MdGT1* may participate in salt stress through anthocyanin antioxidation.

Identification of upstream transcription factor _MdMYB88_

To further determine the regulatory factors involved upstream of *MdGT1*, we conducted the following series of experiments. First, we used bioinformatics to analyze the promoter sequences within 1500 bp upstream of all genes encoding members of the apple glycosyltransferase family (Figure S2a). We selected the myeloblastosis (MYB) binding elements closely related to salt stress and anthocyanin stress (Figure 5a). The related MYB transcription factor was cloned (Tables S5 and S6), and the results of electrophoretic mobility shift assays (EMSA) (Figure 5c) and yeast one-hybrid assay (Figure 5b) identified MdMYB88 as a transcription factor upstream of *MdGT1*.

Gene cloning of the MYB-related elements was performed in the YL and GL strains. After sequencing, it was found that there was a three-base (CCA, Ala) insertion at base 246 (at the 82nd amino acid) in *MdMYB88* in the YL strain. Analysis of its structure revealed that the inserted base was in the HTH domain (between 77-131 amino acids) of *MdMYB88*. We thus speculate that the apple YL mutant may be caused by mutation of the upstream transcription factor *MdMYB88*, which changes its protein function, preventing binding to the promoter sequence of *MdGT1* and thus abolishing regulation of the glycosylation of *MdGT1*.

Related gene expression and proposed working model

The above research showed that *MdGT1* participates in abiotic stress, as well as antioxidant and anthocyanin metabolism. For further analysis of its mechanisms of action, we examined the expression of some stress-related functional genes in *MdGT1* callus by real-time PCR, namely, *MdSOD*, *MdRD22*, *MdRD29A*, *MdRD29B*, *MdMDHA*, *MdDREB1A*, and *MdDREB2B*. *MdDREB1A* and *MdDREB2B* are non-ABA-dependent pathway genes that are regulated by salt induction, *MdRD29A* is a gene related to the ABA-dependent pathway and regulated by salt induction, while the other genes are related to the oxidative stress pathway and their expression is induced and regulated by salt stress (Figure S5). Under normal condition, there is little difference, but after salt stress, the stress-related genes were all upregulated. Compared with transgenic callus, non-transgenic callus has more significant up-regulation of stress-related functional genes. However, upon continued supplementation of the medium with anthocyanin, the stress-related genes were up-regulated significantly in transgenic callus. This may have been because anthocyanins can promote the expression of stress-related genes, reduce the level of active oxygen, and increase the ability to resist stress.

In this study, we propose a working model of the mechanism of action of apple glycosyltransferase *MdGT1* (Figure 6). When a plant is subjected to stress, the stress-related

transcription factor *MdMYB88*, among others, quickly senses the adverse environment and is upregulated, which then attaches to the promoter region of *MdGT1* to regulate its expression. Subsequently, *MdGT1* glycosylates anthocyanin to produce a large amount of 3-O-glucose anthocyanin, which lowers the accumulation of anthocyanin in the plant. As anthocyanin can remove harmful active oxygen from the plant, ultimately the plant's ability to resist salt stress is reduced. In this study, we identified the flavone glycosyltransferase *MdGT1* from apples for the first time, showing that it participates in the regulation of plant stress through the oxidative stress pathway.

Experimental procedures

Plant materials

In terms of the apple material used in this study, the sprout tiller of *M. baccata* started to exhibit YL, as found in the North Homestead of Qingdao Institute of Agricultural Sciences in 2014. In the fall of that year, the branches with YL and GL were cut off and grafted with *M. hupehensis*, which was grown in Shandong Institute of Pomology, Tai'an, Shandong Province, China. In the spring of 2015, the germination of YL and GL was observed, and the length and width of the third leaf, which was selected from the top of the new germination, were measured. The length and thickness of the petiole (diameter) were also measured. Stem diameter and internode length between the third and fourth leaves were also measured from the new germination. The leaves with the same growth state were quickly stored in liquid nitrogen and then sequenced by transcriptome analysis.

Determination of anthocyanin and chlorophyll levels, and western blot

The total anthocyanin and chlorophyll levels in leaves were assayed using the method presented by Wang et al. (2013). Leaves were crushed and pooled to obtain three replicates. Anthocyanin and chlorophyll were extracted in 10 ml of methanol (containing 1% hydrochloric acid) for 2 h at 4℃ in the dark. Anthocyanin and chlorophyll levels were measured at UV at wavelength 553 and 600nm by microplate reader (BIO-RAD 1681130A, California, USA). The anatomical structure of leaves was observed by paraffin sectioning.

To extract total protein from the apple YL and GL tissues, Minute^{TM} total protein extraction kit (Invent SA-01-SK, Shanghai, China) was used, in accordance with the kit's instructions. For western blot analysis of the size of RbcL, at the same time Actin (TransGen Biotech) as the control, the procedure reported by Tien et al. (2019) was follows.

Library construction and transcriptome sequencing

Total RNA was extracted using a modified version of the Hexadecyltrimethy Ammonium Bromide (CTAB) method. RNA quantity and quality (purity and integrity) were analyzed using a NanoPhotometer spectrophotometer (IMPLEN, Westlake Village, CA, USA) and an Agilent Bioanalyzer 2100 system (Agilent Technologies, CA, USA), respectively.

Total RNA from green and yellow cultivars was pooled prior to library preparation in the two experimental groups. Equimolar quantities of total RNA from the samples were combined into a single pool. Prior to cDNA library construction, poly-T oligo-attached magnetic beads were used to purify the mRNA, which was then broken into short fragments of approximately 200 bp. The fragments were used to synthesize first-strand cDNA usingEII. Second-strand cDNA was then synthesized using DNA polymerase I and RNase H. The double-stranded cDNA fragments were subjected to end repair, and sequencing adapters were ligated to both ends. The final cDNA library was selectively enriched by PCR and purified using the AMPure XP system (Beckman Coulter, Beverly, CA, USA). The library preparations were sequenced by Novogene Bioinformatics Technology Co., Ltd. (Beijing, China) on an Illumina HiSeq 2000 platform. Then, 100-bp paired-end reads were generated, and all raw sequence read data were deposited in the NCBI Short Read Archive database under accession number 0000.The BioSample data from NCBI is SAMN16954004.

qRT-PCR analysis

Twenty unigenes were chosen for validation using qRT-PCR. Specific primer pairs for the selected genes used in the qRT-PCR were designed, as shown in Table S5. The cDNA was transcribed from 1 μg of total RNA using *Evo M-MLV* RT Kit with gDNA Clean for qPCR II AG11711 (Accurate Biotechnology (Human) Co.,Ltd) in a reaction mixture with a volume of 20 μL. The qRT-PCR was performed with the ABI 7500 Fast Real-Time Detection System (Applied Biosystems) with the ChamQ Universal SYBR qPCR Master Mix (Vazyme Biotech Co., Ltd). The thermal profile for SYBR Green I RT-PCR was 95°C for 10 min, followed by 40 cycles of 95°C for 15 s and 55°C for 1 min. Each plate was repeated three times in independent runs for all reference and selected genes. A reference gene (β-actin) was used for normalization. The comparative CT method ($2^{-\Delta\Delta CT}$ method) was used to analyze the expression levels of the genes.

Bioinformatic analysis and prediction

Using the SOPMA online software (http://npsapbil.ibcp.fr/cgi-bin/npsa-automat.pl?page=npsa-sopma.html), complete protein secondary structure analysis was performed. In addition,

SWISS MODEL (https://swissmodel.expasy.org/) was used to predict the three-dimensional structure. The amino acid sequences encoded by other glycosyltransferase genes and promoter sequences were downloaded from the NCBI GenBank database. The amino acid sequences of the apple glycosyltransferase family were compared using the software MEGA7 to determine amino acid sequence homology and for the construction of a phylogenetic tree. The locations of the genes in cells were also predicted (http://www.csbio.sjtu.edu.cn/bioinf/Cell-PLoc-2/), as were upstream transcription factors (http://plantpan.itps.ncku.edu.tw/).

Spatiotemporal expression and induction treatment

Regarding analysis of the spatiotemporal expression of genes, the material used was a 10-year-old Malus Purple tree in the North Homestead of Qingdao Institute of Agricultural Sciences. Apple callus was stored in a plant growth room, cultured in a dark room at 25°C, and subcultured every 3 weeks. New roots were obtained, along with annual branches (stems), young leaves and mature leaves, flowers (full blooming period), unbagged skin, and seeds of Malus Purple at 30 and 120 days after flowering. All materials were quickly frozen in nitrogen after sampling, and stored in a –80°C ultra-low-temperature freezer for later use.

For flavonoid induction treatment, apple tree seedlings that normally grow to the six-leaf and one-core stage were obtained, and the roots were placed in 100 μmol/L quercetin, kaempferol, and anthocyanin solution. For abiotic stress induction treatment, apple tree seedlings that normally grow to the six-leaf and one-core stage were obtained, and the roots were placed in 150 mM NaCl, 100 μM ABA, and 250 mM mannitol solution at 4°C for 1, 3, 6, 12, or 24 h. After the treatment, all materials were quickly frozen in liquid nitrogen after sampling, and stored in an ultra-low-temperature freezer at –80℃ for later use.

***In vitro* enzymatic reaction and HPLC analysis**

The collection of bacteria was performed in accordance with the paper by Li et al. (2017). For protein purification, the GST-tagged protein on the prokaryotic expression vector could be successfully eluted by binding to agarose beads Glutathione Sephrose 4B (purchased from General Electric Company). The specific method was performed in accordance with the work of Li et al. (2019), after which the active enzyme was obtained.

For the *in vitro* enzymatic reaction, the reaction system is shown in Table S1. The specific

operation steps were performed in accordance with the work of Li et al. (2019).

According to the reaction system (Table S1), the reaction was allowed to proceed for different times or with different substrate concentrations in a 30℃ water bath. For the reaction at the optimal temperature and pH value, enzyme activity was analyzed according to the HPLC peak value.

The HPLC analytical instrument was a Shimadzu LC-20AT (Shimadzu, Japan). Regarding the HPLC analysis conditions, the mobile phase of flavonoids was acetonitrile (mobile phase A) and 0.1% trifluoroacetic acid (mobile phase B). Using a binary high-pressure concentration gradient method for elution, the flow rate was 1 ml/min, elution time was 35 min, with the following set program: 0 min B phase 90%, 20 min B phase 25%, 22 min B phase 90%, and 35 min stop. For flavonoid detection, the wavelength was 270 nm. The LC-MC analytical instrument was a Surveyor MSQ (USA) single-quadrupole liquid chromatography mass spectrometer.

Vector construction and transgenic apple callus strains

For vector construction, all reaction solutions were prepared on ice, with reference to the kits' instructions for the specific steps. The kit used for gene cloning was purchased from Dalian TakaRa Bioengineering Co., Ltd. (catalog number R011). The intermediate carrier pZero Blunt Simple was purchased from Beijing Quanshijin Biotechnology Co., Ltd. (catalog number CB101). *Escherichia coli* plasmid extraction was performed using Tiangen Plasmid Extraction Kit, purchased from Tiangen Biochemical Technology Co., Ltd. (Beijing, China; catalog number DP103-03).

For establishment of the transgenic apple callus, before transformation, the required callus was prepared and cultured for 10–15 days after subculture, followed by selection for transformation (Liu et al., 2020).

Determination of related physiological indicators

For determination of the ROS level of callus, a ROS determination kit (Plant ROS Elisa Kit, Beijing Dongge, CK -E0071P) was used, in accordance with the manufacturer's instructions.

For determination of the total antioxidant capacity of callus, a total antioxidant capacity test kit (FRAP method, production lot number S0116) was used, in accordance with the manufacturer's instructions.

The determination of proline content was performed in accordance with a conventional internationally accepted method (Li et al., 2015). The determination of soluble sugar content was performed following the previously reported, internationally accepted anthrone method (Li et al.,

2017).

Adversity stress treatment

The apple callus with uniform growth was cultured on medium containing 100 mM NaCl, 10 μM anthocyanin, 100 mM NaCl, and 10 μM anthocyanin for 2 weeks. Normal medium was used as a control for observation to compare the growth statuses of the calluses, by determining their fresh weights.

Electrophoretic mobility shift assay

Bioinformatics was used to predict and analyze the possible binding of transcription factors upstream of MdGT1. After screening, recombinant *MdMYB111 (LOC103403724), MdMYB46 (LOC103427345), MdMYB74 (LOC103422412), MdRVE8 (LOC103450146), MdMYB306 (LOC103442350), MdMYB20 (LOC103444230), MdMYB58 (LOC103435557), MdMYB88 (LOC103402919), MdMYB44 (LOC103453725), MdMYB59 (LOC103421497),* and *MdMYB308 (LOC103440814)* proteins fused with His-tag were expressed in *E. coli* (BL21/DE3) and purified with Ni-NTA columns. Biotin-labeled DNA probes are listed in Supplemental Table S5. The specific method was performed in accordance with the EMSA kit instructions (Thermo Scientific, USA, 89818).

Yeast one-hybrid screening

For preparation of competent yeast, the method reported by Miller et al. (2019) was used. For yeast co-transformation, more than 200 ng of DNA-binding domain carrier (pLacZi2u-pMdGT1) and DNA-activation carrier (pJG4-5-MdMYB88), and 100 μL of the prepared competent yeast were added to a 1.5 mL centrifuge tube. See Miller et al. (2019) for the specific yeast transformation steps.

For the determination of β-galactosidase, the fusion yeast in the yeast one-hybrid culture was cultured overnight at 28°C on selective medium. A single colony was selected and cultured overnight in 3 mL of SD (glucose) medium. The next day, it was replaced with SD (galactose and raffinose) medium. After incubation, the activity of β-galactosidase was measured, in accordance with the method described by Miller et al. (2019).

Statistical analysis

All experiments were performed as three independent biological replicates, with at least three technical replicates established each time. The significance of differences between each experimental sample and the control sample was tested using Student's *t*-test. Differences at $^{*}P < 0.05$ were considered significant, while differences at $^{**}P < 0.01$ were considered extremely significant.

Author contributions

S.Z., L.J., and G.S. conceived the original screening and research plans; P.L., H.G., L.Z., J.S., and Z.S. performed experiments, analyzed the data, made the figures, and wrote the original article; L.J., C.Z., and H.S. provided suggestions; P.L. and S.Z. supervised and complemented the writing. All authors read and approved the final manuscript.

Conflict of interest

The authors declare that they have no conflicts of interest.

Acknowledgement

This project was supported by grants from the National Natural Science Foundation of China (Grant No. 32001982, 31972357, 31801821, and 31772254), Shandong Provincial Natural Science Foundation of China (Grant No. ZR2019PC041), National Key Research and Development Program of China (2019YFD1000104, SQ2020YFF0422322). Supported by the Open Project Program (2020KF09) of State Key Laboratory of Crop Biology, SDAU, Tianan, Shandong.

Supporting information

Figure S1

(a) Different colors represent different amino acid sequences.

(b) Analysis of the physicochemical properties of 34 apple glycosyltransferases.

Figure S2

(a) Bioinformatics was used to analyze the promoter sequences within 1500 bp upstream of 34 apple glycosyltransferase family genes.

(b) Temporal and spatial expression of 34 apple glycosyltransferase family genes.

Figure S3

Abiotic stress-induced expression of 34 apple glycosyltransferase family genes.

Figure S4

Specific activity of *MdGT1* to different substrates.

Table S1

In vitro enzymatic reaction system

Table S2

Plant glycosyltransferase conserved amino acid sequence (44 bases)

Table S3

MdGT1 gene CDS sequences

Table S4

MdGT1 amino acid sequences

Table S5

Related gene primers

Table S6

CDS sequences of *MdMYB* transcription factors

References

Burgess, D.J. (2017) Genetic engineering: CREATE-ing genome-wide designed mutations. *Nat. Rev. Genet.* 18, 69.

Cassidy, A. and Minihane, A.M. (2017) The role of metabolism (and the microbiome) in defining the clinical efficacy of dietary flavonoids. *Am. J. Clin. Nutr.* 105, 10-22.

Champeyroux, C., Bellati, J., Barberon, M., Rofidal, V., Maurel, C. and Santoni, V. (2019) Regulation of a plant aquaporin by a Casparian strip membrane domain protein-like. *Plant Cell Environ*. 42, 1788-1801.

Dare, A.P., Yauk, Y.K., Tomes, S., McGhie, T.K., Rebstock, R.S., Cooney, J.M. and Atkinson, R.G. (2017) Silencing a phloretin-specific glycosyltransferase perturbs both general phenylpropanoid biosynthesis and plant development. *Plant J.* 91, 237-250.

Elejalde-Palmett, C., Billet, K., Lanoue, A., De Craene, J.O., Glévarec, G., Pichon, O., Clastre, M., Courdavault, V., St-Pierre, B., Giglioli-Guivarc'h, N., Dugé de Bernonville, T. and Besseau, S. (2019) Genome-wide identification and biochemical characterization of the UGT88F subfamily in Malus x domestica Borkh. *Phytochemistry.* 157, 135-144.

Gachon, C.M.M., Langlois-Meurinne, M., Henry, Y. and Saindrenan, P. (2005) Transcriptional co-regulation of secondary metabolism enzymes in Arabidopsis: functional and evolutionary implications. *Plant Mol. Biol.* 58, 229-245.

Harborne, J.B. and Williams, C.A. (2000) Advances in flavonoid research since 1992. *Phytochemistry.* 55, 481-504.

Hingst, J.R., Bruhn, L., Hansen, M.B., Rosschou, M.F., Birk, J.B., Fentz, J., Foretz, M., Viollet, B., Sakamoto, K., Færgeman, N.J., Havelund, J.F., Parker, B.L., James, D.E., Kiens, B., Richter, E.A., Jensen, J. and Wojtaszewski, J.F.P. (2018) Exercise-induced molecular mechanisms promoting glycogen supercompensation in human skeletal muscle. *Mol. Metab.* 16, 24-34.

Li, P., Lei, K., Li, Y., He, X., Wang, S., Liu, R., Ji, L. and Hou, B. (2019) Identification and characterization of the first cytokinin glycosyltransferase from rice. *Rice (N Y).* 12, 19-30.

Li, P., Li, Y.J., Zhang, F.J., Zhang, G.Z., Jiang, X.Y., Yu, H.M. and Hou, B.K. (2017) The Arabidopsis UDP-glycosyltransferases UGT79B2 and UGT79B3 contribute to cold, salt and drought stress tolerance via modulating anthocyanin accumulation. *Plant J*. 89, 85-103.

Lin, J.S., Huang, X.X., Li, Q., Cao, Y., Bao, Y., Meng, X.F., Li, Y.J., Fu, C. and Hou, B.K. (2016) UDP-glycosyltransferase 72B1 catalyzes the glucose conjugation of monolignols and is essential for the normal cell wall lignification in Arabidopsis thaliana. *Plant J.* 88, 26-42.

Li, Y.J., Wang, B., Dong, R.R. and Hou, B.K. (2015) AtUGT76C2, an Arabidopsis cytokinin glycosyltransferase is involed in drought stress adaptation. *Plant Sci.* 236, 157-167.

Liu, L., Yu, Z.P., Xu, Y., Guo, C., Zhang, L., Wu, C.G., Yang, G.D., Huang, J.G., Yan, K., Shu, H.R., Zheng, C.C. and Zhang, S.Z. (2020) Function identification of MdTIR1 in apple root growth benefited from the predicted MdPPI network. *J. Integr. Plant Biol.* 2020, 1-17.

Liu, Z., Yan, J.P., Li, D.K., Luo, Q., Yan, Q., Liu, Z.B., Ye, L.Y., Wang, J.M., Li, X.F. and Yang, Y. (2015) UDP-glucosyltransferase71c5, a major glucosyltransferase, mediates abscisic acid homeostasis in Arabidopsis. *Plant Physiol.* 167, 1659-1670.

Ma, H., Johnson, S.L., Liu, W., DaSilva, N.A., Meschwitz, S., Dain, J.A. and Seeram, N.P. (2018) Evaluation of polyphenol anthocyanin-enriched extracts of blackberry, black raspberry, blueberry, cranberry, red raspberry, and strawberry for free radical scavenging, reactive carbonyl species trapping, anti-glycation, anti-β-amyloid aggregation, and microglial neuroprotective effects. *Int. J. Mol. Sci.* 19, 461.

Meyer, P., Heidmann, I., Forkmann, G. and Saedler, H. (1987) A new petunia flower colour generated by transformation of a mutant with a maize gene. *Nature*. 330, 677-678.

Miller, T.C.R., Locke, J., Greiwe, J.F., Diffley, J.F.X. and Costa, A. (2019) Mechanism of head-to-head MCM double-hexamer formation revealed by cryo-EM. *Nature*. 575, 704-710.

Pospisil, P. (2012) Molecular mechanisms of production and scavenging of reactive oxygen species by

photosystem II. *Biochim. Biophys. Acta*. *Biomembr.* 1817, 218-231.

Scuffi, D., Alvarez, C., Laspina, N., Gotor, C., Lamattina, L. and Garcia, M. (2014) Hydrogen sulfide generated by L-cysteine desulfhydrase acts upstream acid-dependent stomatal closure. *Plant Physiol*. 166, 2065-2076.

Sun, Y.G., Wang, B., Jin, S.H., Qu, X.X., Li, Y.J. and Hou, B.K. (2013) Ectopic expression of Arabidopsis glycosyltransferase UGT85A5 enhances salt stress tolerance in tobacco. *PLoS One*. 8, e59924.

Tawfeek, N., Sobeh, M., Hamdan, D.I., Farrag, N., Roxo, M., El-Shazly, A.M. and Wink, M. (2019) Phenolic compounds from populus alba L. and salix subserrata willd. (Salicaceae) counteract oxidative stress in caenorhabditis elegans. *Molecules*. 24, 1999-2018.

Tien, N.Q., Huy, N.X. and Kim, M.Y. (2019) Improved expression of porcine epidemic diarrhea antigen by fusion with cholera toxin B subunit and chloroplast transformation in Nicotiana tabacum. *Plant Cell Tissue Organ Cult.* 137, 213-223.

Tognetti, V.B., Van Aken, O., Morreel, K., Vandenbroucke, K., van de Cotte, B., De Clercq, I., Chiwocha, S., Fenske, R., Prinsen, E., Boerjan, W., Genty, B., Stubbs, K.A., Inzé, D. and Van Breusegem, F. (2010) Perturbation of indole-3-butyric acid homeostasis by the UDP-glucosyltransferase UGT74E2 modulates Arabidopsis architecture and water stress tolerance. *Plant Cell.* 22, 2660-2679.

Vanderzande, S., Howard, N.P., Cai, L., Da Silva Linge, C., Antanaviciute, L., Bink, M.C.A.M., Kruisselbrink, J.W., Bassil, N., Gasic, K., Iezzoni, A., Van de Weg, E. and Peace, C. (2019) High-quality, genome-wide SNP genotypic data for pedigreed germplasm of the diploid outbreeding species apple, peach, and sweet cherry through a common workflow. *PLoS One.* 14,e0210928.

Velasco, R., Zharkikh, A., Affourtit, J., Dhingra, A., Cestaro, A., Kalyanaraman, A., Fontana, P., Bhatnagar, S.K., Troggio, M., Pruss, D., Salvi, S., Pindo, M., Baldi, P., Castelletti, S., Cavaiuolo, M., Coppola, G., Costa, F., Cova, V., Dal Ri, A., Goremykin, V., Komjanc, M., Longhi, S., Magnago, P., Malacarne, G., Malnoy, M., Micheletti, D., Moretto, M., Perazzolli, M., Si-Ammour, A., Vezzulli, S., Zini, E., Eldredge, G., Fitzgerald, L.M., Gutin, N., Lanchbury, J., Macalma, T., Mitchell, J.T., Reid, J., Wardell, B., Kodira, C., Chen, Z., Desany, B., Niazi, F., Palmer, M., Koepke, T., Jiwan, D., Schaeffer, S., Krishnan, V., Wu, C.,

Chu, V.T., King, S.T., Vick, J., Tao, Q., Mraz, A., Stormo, A., Stormo, K., Bogden, R., Ederle, D., Stella, A., Vecchietti, A., Kater, M.M., Masiero, S., Lasserre, P., Lespinasse, Y., Allan, A.C., Bus, V., Chagné, D., Crowhurst, R.N., Gleave, A.P., Lavezzo, E., Fawcett, J.A., Proost, S., Rouzé, P., Sterck, L., Toppo, S., Lazzari, B., Hellens, R.P., Durel, C.E., Gutin, A., Bumgarner, R.E., Gardiner, S.E., Skolnick, M., Egholm, M., Van de Peer, Y., Salamini, F. and Viola, R. (2010) The genome of the domesticated apple (Malus×domestica Borkh.). *Nat. Genet.* 42, 833-839.

Verma, V., Ravindran, P. and Kumar, P.P. (2016) Plant hormone-mediated regulation of stress response. *BMC Plant Biol.* 16, 86-96.

Vyacheslav, K., Suleyman, A. and Serguei, Z. (2000) Shortening of life-time of the pair [P680+Pheo-] contributes to general inhibitory effect of dinoseb on electron transfer in PS-II. *Indian J. Biochem. Biophys.* 37, 491-497.

Wang, H., Zhang, H., Yang, Y., Li, M., Zhang, Y., Liu, J., Dong, J., Li, J., Butelli, E., Xue, Z., Wang, A., Wang, G., Martin, C. and Jin, W. (2020) The control of red colour by a family of MYB transcription factors in octoploid strawberry (Fragaria ananassa) fruits. *Plant Biotechnol. J.* 18, 1169-1184.

Wang, L.S., Zhao, C., Gu, Y., Zhou, H., Zhou, J., Ma, J. and Cheng, Y.H. (2013) Deep RNA-Seq uncovers the peach transcriptome landscape. *Plant Mol. Biol.* 83, 365-377.

Wang, P., Li, Z., Wei, J., Zhao, Z., Sun, D., and Cul, S. (2012) A Na+/Ca+ exchanger-like protein(AtNCL) involved in salt stress in Arabidopsis. *J. Biol. Chem.* 287, 44062-44070.

Winkel-Shirley, B. (2001) It takes a garden. How work on diverse plant species has contributed to an understanding of flavonoid metabolism. *Plant Physiol.* 127, 1399-1404.

Xie, Y.P., Chen, P.X., Yan, Y., Bao, C.N., Li, X.W., Wang, L.P., Shen, X.X., Li, H.Y., Liu, X.F., Niu, C.D., Zhu, C., Fang, N., Shao, Y., Zhao, T., Yu, J.T., Zhu, J.H., Xu, L.F., van Nocker, S., Ma, F.W. and Guan, Q.M. (2018) An atypical R2R3 MYB transcription factor increases cold hardiness by CBF-dependent and CBF-independent pathways in apple. *New Phytol.* 218, 201-218.

Yahyaa, M., Davidovich-Rikanati, R., Eyal, Y., Sheachter, A., Marzouk, S., Lewinsohn, E. and Ibdah, M. (2016) Identification and characterization of UDP-glucose:Phloretin 4'-O-glycosyltransferase from Malus x domestica Borkh. *Phytochemistry.* 130, 47-55.

Yin, R.H., Kerstin, H., Werner, H., Andreas, A., Petre, I.D., Eva, Z. and Schäffner, A.R. (2013)

Kaempferol-3-O-rhamnoside-7-O-rhamnoside is an endogenous flavonol inhibitor of polar auxin transport in Arabidopsis shoots. *New Phytol*. 201, 466-475.

Yonekura-Sakakibara, K., Tohge, T., Matsudam, F., Nakabayashi, R., Takayama, H., Niida, R., Watanabe-Takahashi, A., Inoue, E. and Saito, K. (2008) Comprehensive flavonol profiling and transcriptome coexpression analysis leading to decoding gene-metabolite correlations in arabidopsis. *Plant Cell.* 20, 2160-2176.

Yonekura-Sakakibara, K., Nakabayashi, R., Sugawara, S., Tohge, T., Ito, T., Koyanagi, M., Kitajima, M., Takayama, H. and Saito, K. (2014) A flavonoid 3-O-glucoside:2″-O-glucosyltransferase responsible for terminal modification of pollen-specific flavonols in Arabidopsis thaliana. *Plant J.* 79, 769-782.

Zhang, Y., Su, J., Cheng, D., Wang, R., Mei, Y., Hu, H., Shen, W., Zhang, Y. (2018) Nitric oxide contributes to methane-induced osmotic stress tolerance in mung bean. *BMC Plant Biol.* 18, 207.

Zhao, M., Li, J., Zhu, L., Chang, P., Li, L. and Zhang, L. (2019) Identification and characterization of MYB-bHLH-WD40 regulatory complex members controlling anthocyanidin biosynthesis in blueberry fruits development. *Genes (Basel).* 10, 496-507.

Zhou, K., Hu, L., Li, P., Gong, X. and Ma, F. (2017) Genome-wide identification of glycosyltransferases converting phloretin to phloridzin in Malus species. *Plant Sci.* 265, 131-145.

Figure legends

Figure 1. Observation of biological characteristics

(a) Phenotype comparison between normal apple branches and yellow mutant apple branches.

(b) The length and width of the third leaf, which was selected from the top of the new germination, were measured.

(c) The branches with yellow and green leaves (YL and GL) were cut off and grafted with *Malus hupehensis*, grown in Shandong Institute of Pomology, Tai'an, Shandong Province, China.

(d) The main veins of leaves of YL and GL were observed by HE staining under a microscope: left (20×) and right (40×).

(e) The levels of chlorophyll a, b, carotenoid, and anthocyanin in YL and GL measured by a UV spectrophotometer.

(f) Western blot detected the chloroplast protein subunits of YL and GL.

Figure 2. Transcriptome sequencing between yellow and green leaves (YL and GL) lines

(a) The number of upregulated and downregulated unigenes between YL and GL lines.

(b) Sequences annotated to the canonical reference pathways in the KEGG database.

(c) Flavonoid biosynthesis pathway.

(d) Expression of genes related to the flavonoid biosynthesis pathway and five glycosyltransferase genes.

Figure 3. Analysis of sequence information of *MdGT1* and enzyme activity identification In vitro

(a) Construction of apple glycosyltransferase gene evolutionary tree by MEGA7.0.

(b) Bioinformatic analysis and comparison of all apple glycosyltransferase gene sequences.

(c) *MdGT1* expression pattern.

(d) *MdGT1* induced expression by 150 mM NaCl, 100 μM ABA, 250 mM mannitol, and a temperature of 4℃ for 1, 3, 6, 12, and 24 h.

(e) *MdGT1* expression induced by 100 μM/L anthocyanin, quercetin, and kaempferol for 1, 3, 6, 12, and 24 h.

(f) HPLC analysis of reaction products from anthocyanin catalyzed by MdGT1.

(g) HPLC analysis of reaction products from quercetin catalyzed by *MdGT1*.

(h) HPLC analysis of reaction products from kaempferol catalyzed by *MdGT1*.

Figure 4 Expression intensity of *MdGT1 OE* lines and their phenotype

(a) Expression intensity of *MdGT1 OE* lines, as *OE4* upregulated 14.72 times, *OE9* upregulated 15.38 times, and *OE15* upregulated 15.01 times.

(b) Phenotypic observation of *MdGT1 OE4*, *OE9*, and *OE15* under 100 mM NaCl, 20 μM anthocyanin, and 100 mM NaCl+20 μM anthocyanin treatment.

(c) Bioaccumulation statistics.

(d) Anthocyanin content determination.

(e) ROS content determination.

(f) Antioxidant activity determination.

(g) Glutathione content determination.

(h) Ascorbate content determination.

Figure 5 *MdGT1* upstream transcription factor determination

(a) *MdGT1* promoter sequence analysis, including five MYB binding elements: P1 (–1200 bp to –1180 bp), P2 (–796 bp to –775 bp), P3 (–1200 bp to –1180 bp), P4 (–613 bp to –598 bp), and P5 (–200 bp to –189 bp).

(b) Interaction of *MdGT1* promoter elements with the *MdMYB88* transcription factor evaluated by yeast one-hybrid assays; probes –200 bp to –189 bp containing the *MdMYB* sequences within the *MdGT1* promoter were synthesized and employed for this assay.

(c) Interaction of *MdGT1* promoter elements with the *MdMYB88* transcription factor as shown by electrophoretic mobility shift assays (EMSA); probes –200 bp to –189 bp containing the *MdMYB* element within the *MdGT1* promoter were synthesized and employed for this assay.

Figure 6 *MdGT1* working model

MdMYB88 sense the adverse environment and is upregulated, which then attaches to the promoter region of *MdGT1*. Subsequently, MdGT1 glycosylates anthocyanin, which lowers the accumulation of anthocyanin in the plant. As anthocyanin can remove harmful active oxygen from the plant, ultimately the plant's ability to resist salt stress is reduced.

Figure 1

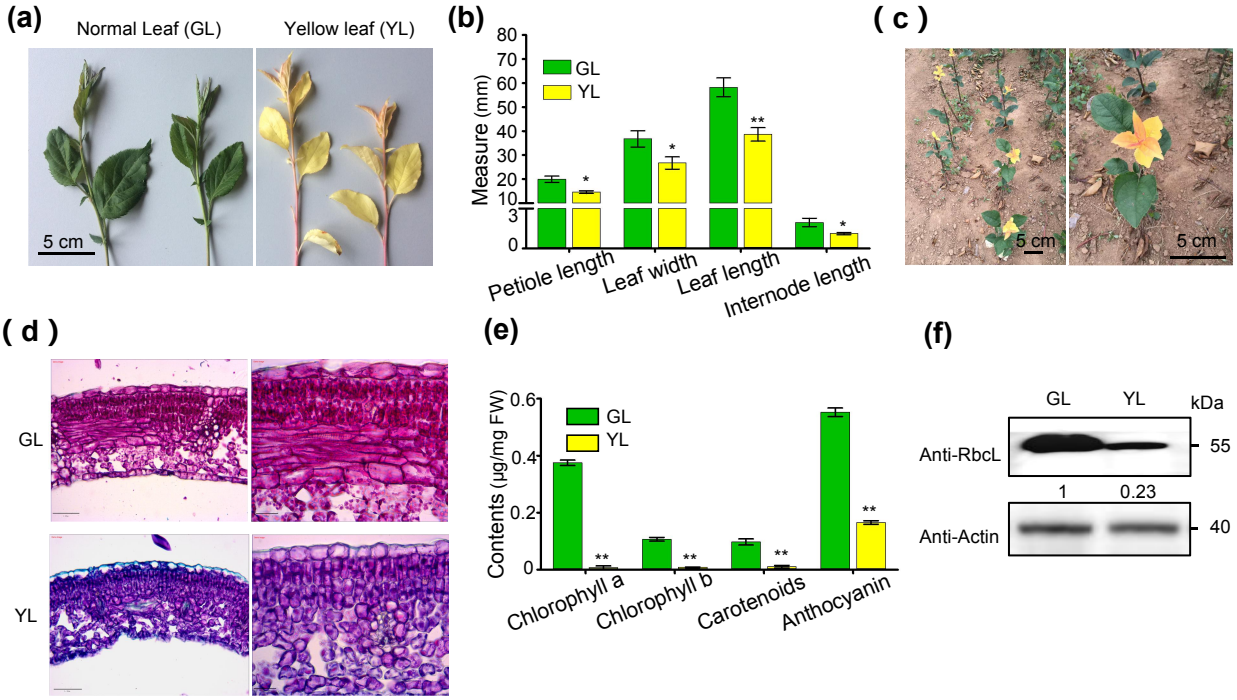
(a)
Normal Leaf (GL)
Yellow leaf (YL)
5 cm
(b)
Measure (mm)
GL
YL
Petiole length
Leaf width
Leaf length
Internode length
(c)
5 cm
5 cm
(d)
GL
YL
(e)
Contents (μg/mg FW)
GL
YL
Chlorophyll a
Chlorophyll b
Carotenoids
Anthocyanin
(f)
GL
YL
kDa
Anti-RbcL
55
1
0.23
Anti-Actin
40

Figure 2

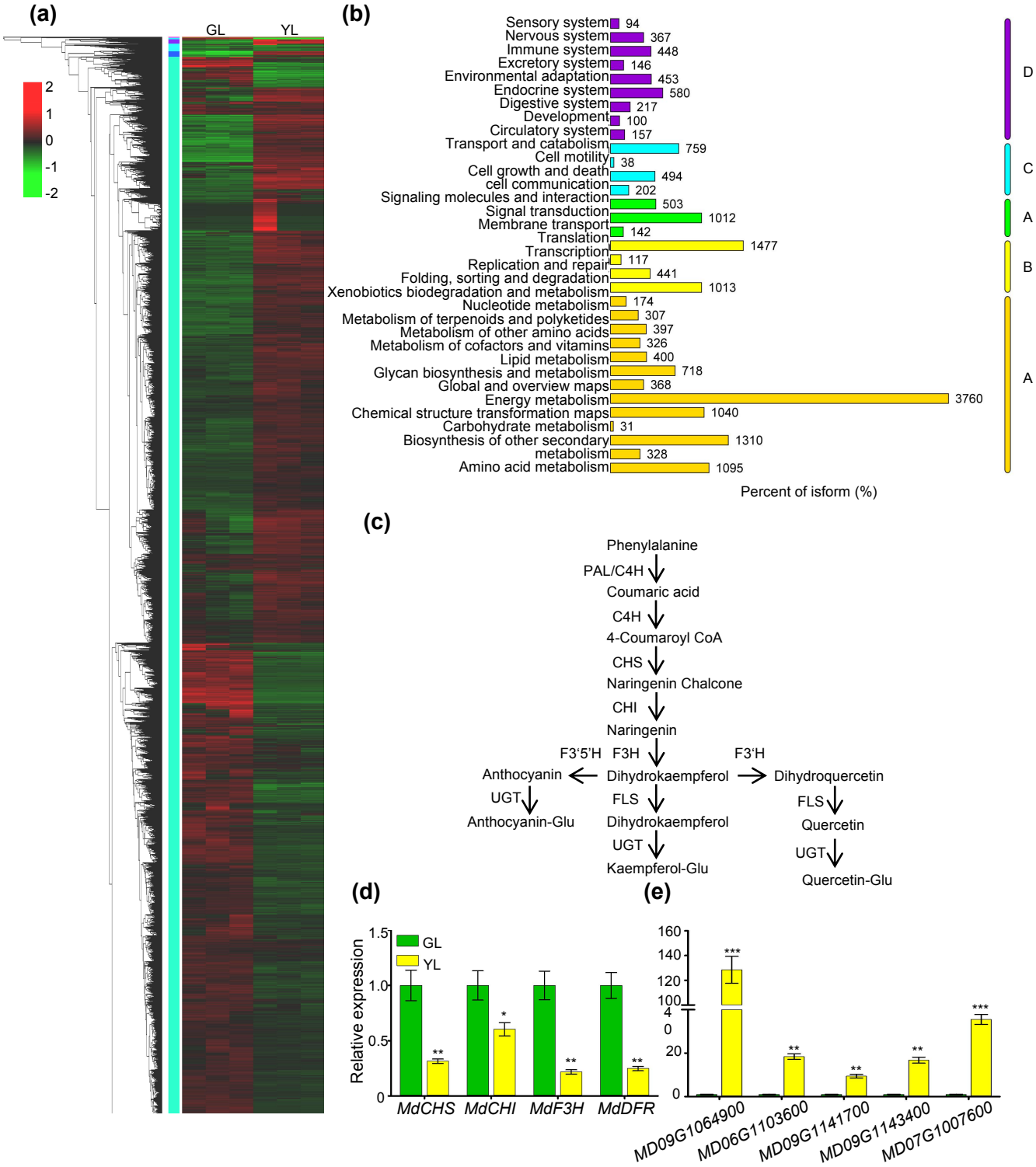
(a)
GL
YL
2
1
0
-1
-2
(b)
Sensory system 94
Nervous system 367
Immune system 448
Excretory system 146
Environmental adaptation 453
Endocrine system 580
Digestive system 217
Development 100
Circulatory system 157
Transport and catabolism 759
Cell motility 38
Cell growth and death 494
cell communication 202
Signaling molecules and interaction 503
Signal transduction 1012
Membrane transport 142
Translation 1477
Transcription 117
Replication and repair 441
Folding, sorting and degradation 1013
Xenobiotics biodegradation and metabolism 174
Nucleotide metabolism 307
Metabolism of terpenoids and polyketides 397
Metabolism of other amino acids 326
Metabolism of cofactors and vitamins 400
Lipid metabolism 718
Glycan biosynthesis and metabolism 368
Global and overview maps 3760
Energy metabolism 1040
Chemical structure transformation maps 31
Carbohydrate metabolism 1310
Biosynthesis of other secondary metabolism 328
Amino acid metabolism 1095
Percent of isform (%)
D
C
A
B
A
(c)
Phenylalanine
PAL/C4H
Coumaric acid
C4H
4-Coumaroyl CoA
CHS
Naringenin Chalcone
CHI
Naringenin
F3'5'H
F3H
F3'H
Anthocyanin
Dihydrokaempferol
Dihydroquercetin
UGT
FLS
FLS
Anthocyanin-Glu
Dihydrokaempferol
Quercetin
UGT
UGT
Kaempferol-Glu
Quercetin-Glu
(d)
Relative expression
GL
YL
1.5
1.0
0.5
0
MdCHS
MdCHI
MdF3H
MdDFR
(e)
160
140
120
100
4
0
20
0
MD09G1064900
MD06G1103600
MD09G1141700
MD09G1143400
MD07G1007600

Figure 3

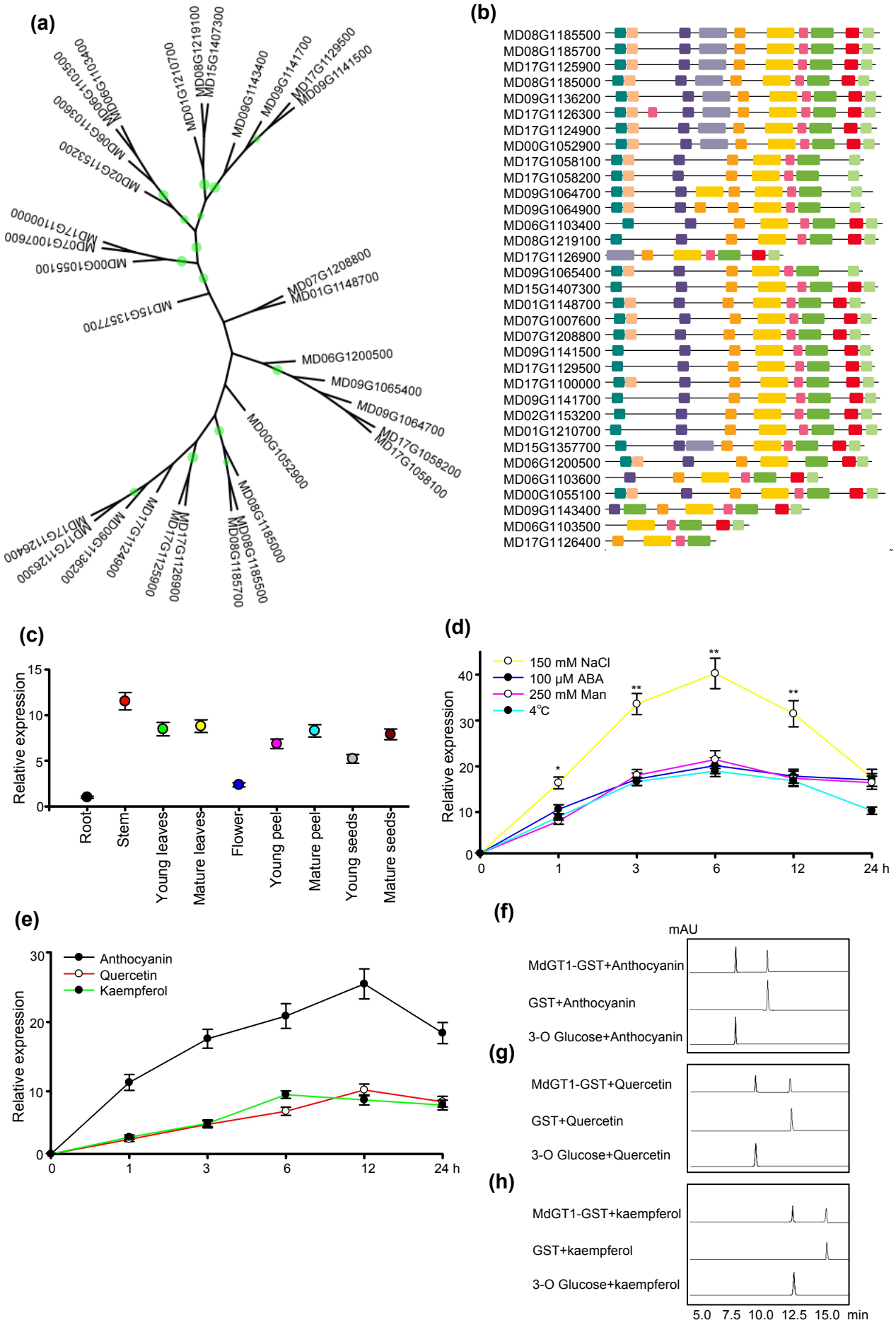
(a)
MD01G1210700
MD08G1219100
MD15G1407300
MD09G1143400
MD09G1141700
MD17G1129500
MD09G1141500
MD06G1103400
MD06G1103500
MD06G1103600
MD02G1153200
MD17G1100000
MD07G1007600
MD00G1055100
MD15G1357700
MD07G1208800
MD01G1148700
MD06G1200500
MD09G1065400
MD09G1064700
MD17G1058200
MD17G1058100
MD00G1052900
MD08G1185000
MD08G1185500
MD08G1185700
MD17G1126900
MD17G1125900
MD09G1136200
MD17G1124900
MD17G1126400
(b)
MD08G1185500
MD08G1185700
MD17G1125900
MD08G1185000
MD09G1136200
MD17G1126300
MD17G1124900
MD00G1052900
MD17G1058100
MD17G1058200
MD09G1064700
MD09G1064900
MD06G1103400
MD08G1219100
MD17G1126900
MD09G1065400
MD15G1407300
MD01G1148700
MD07G1007600
MD07G1208800
MD09G1141500
MD17G1129500
MD17G1100000
MD09G1141700
MD02G1153200
MD01G1210700
MD15G1357700
MD06G1200500
MD06G1103600
MD00G1055100
MD09G1143400
MD06G1103500
MD17G1126400
(c)
Relative expression
Root
Stem
Young leaves
Mature leaves
Flower
Young peel
Mature peel
Young seeds
Mature seeds
(d)
150 mM NaCl
100 μM ABA
250 mM Man
4℃
Relative expression
24 h
(e)
Anthocyanin
Quercetin
Kaempferol
Relative expression
24 h
(f)
mAU
MdGT1-GST+Anthocyanin
GST+Anthocyanin
3-O Glucose+Anthocyanin
(g)
MdGT1-GST+Quercetin
GST+Quercetin
3-O Glucose+Quercetin
(h)
MdGT1-GST+kaempferol
GST+kaempferol
3-O Glucose+kaempferol
5.0 7.5 10.0 12.5 15.0 min

Figure 4

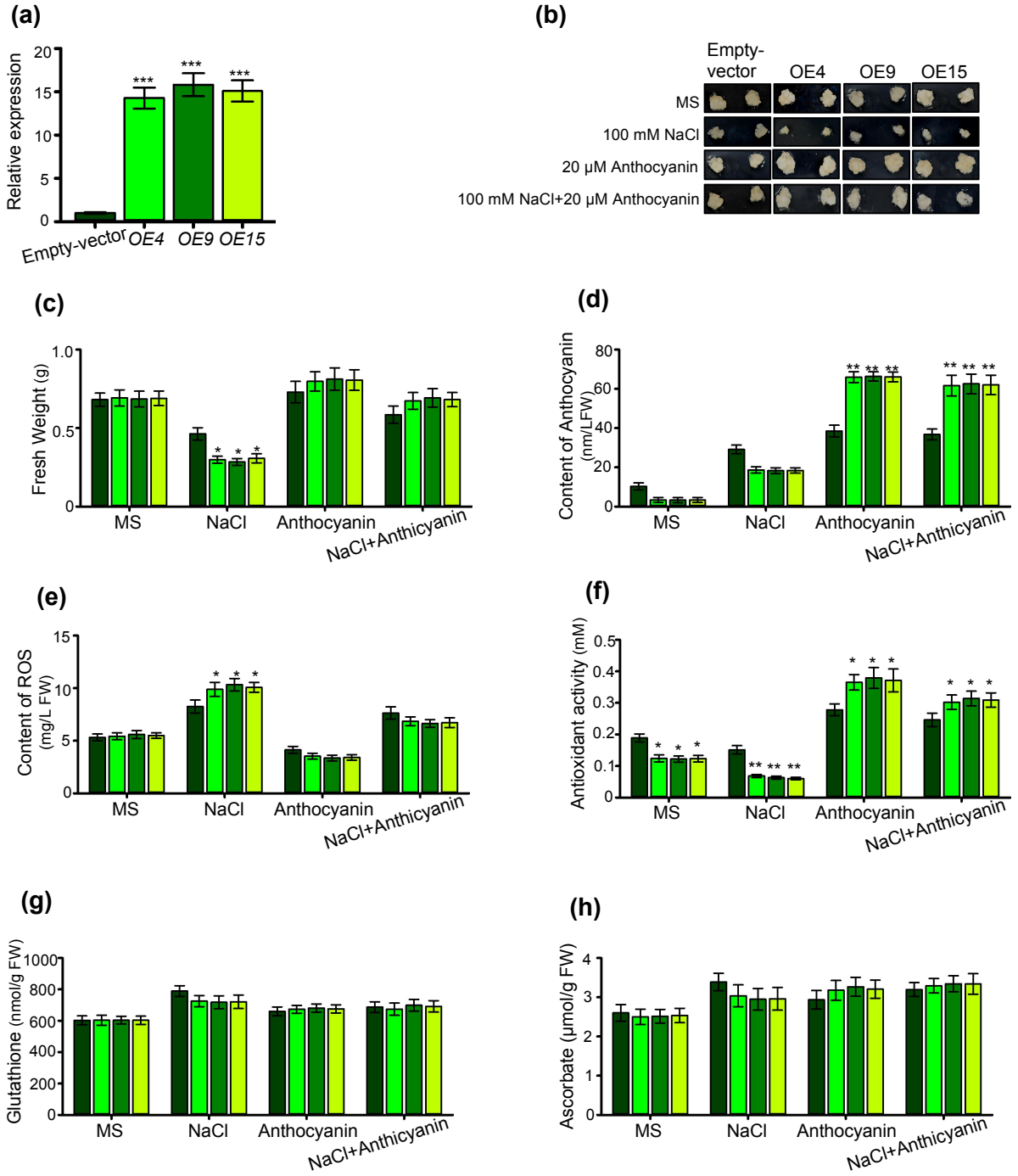
(a)
Relative expression
20
15
10
5
0
***
***
***
Empty-vector
OE4
OE9
OE15
(b)
Empty-vector
OE4
OE9
OE15
MS
100 mM NaCl
20 μM Anthocyanin
100 mM NaCl+20 μM Anthocyanin
(c)
Fresh Weight (g)
1.0
0.5
0
MS
NaCl
Anthocyanin
NaCl+Anthicyanin
(d)
Content of Anthocyanin (nm/LFW)
80
60
40
20
0
MS
NaCl
Anthocyanin
NaCl+Anthicyanin
(e)
Content of ROS (mg/L FW)
15
10
5
0
MS
NaCl
Anthocyanin
NaCl+Anthicyanin
(f)
Antioxidant activity (mM)
0.5
0.4
0.3
0.2
0.1
0
MS
NaCl
Anthocyanin
NaCl+Anthicyanin
(g)
Glutathione (nmol/g FW)
1000
800
600
400
200
0
MS
NaCl
Anthocyanin
NaCl+Anthicyanin
(h)
Ascorbate (μmol/g FW)
4
3
2
1
0
MS
NaCl
Anthocyanin
NaCl+Anthicyanin

Figure5

(a)

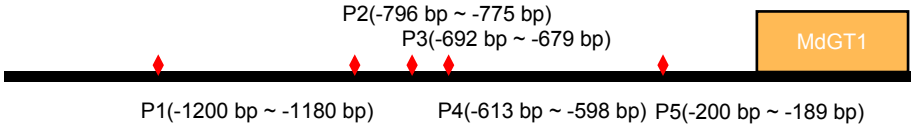

(b)

Positive Control	
P5+Empty vector	P5+MdMYB88
P4+Empty vector	P4+MdMYB88
P3+Empty vector	P3+MdMYB88
P2+Empty vector	P2+MdMYB88
P1+Empty vector	P1+MdMYB88

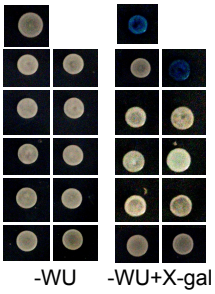

(c)

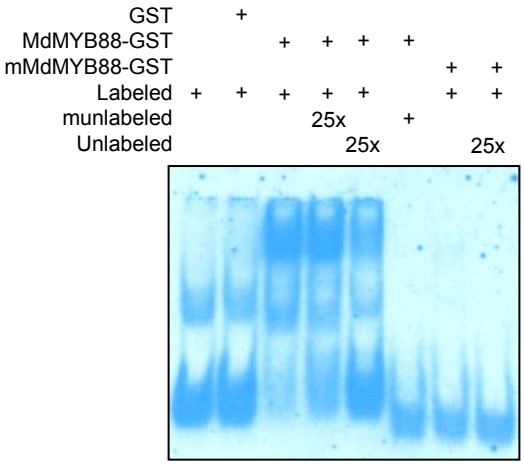

Figure6

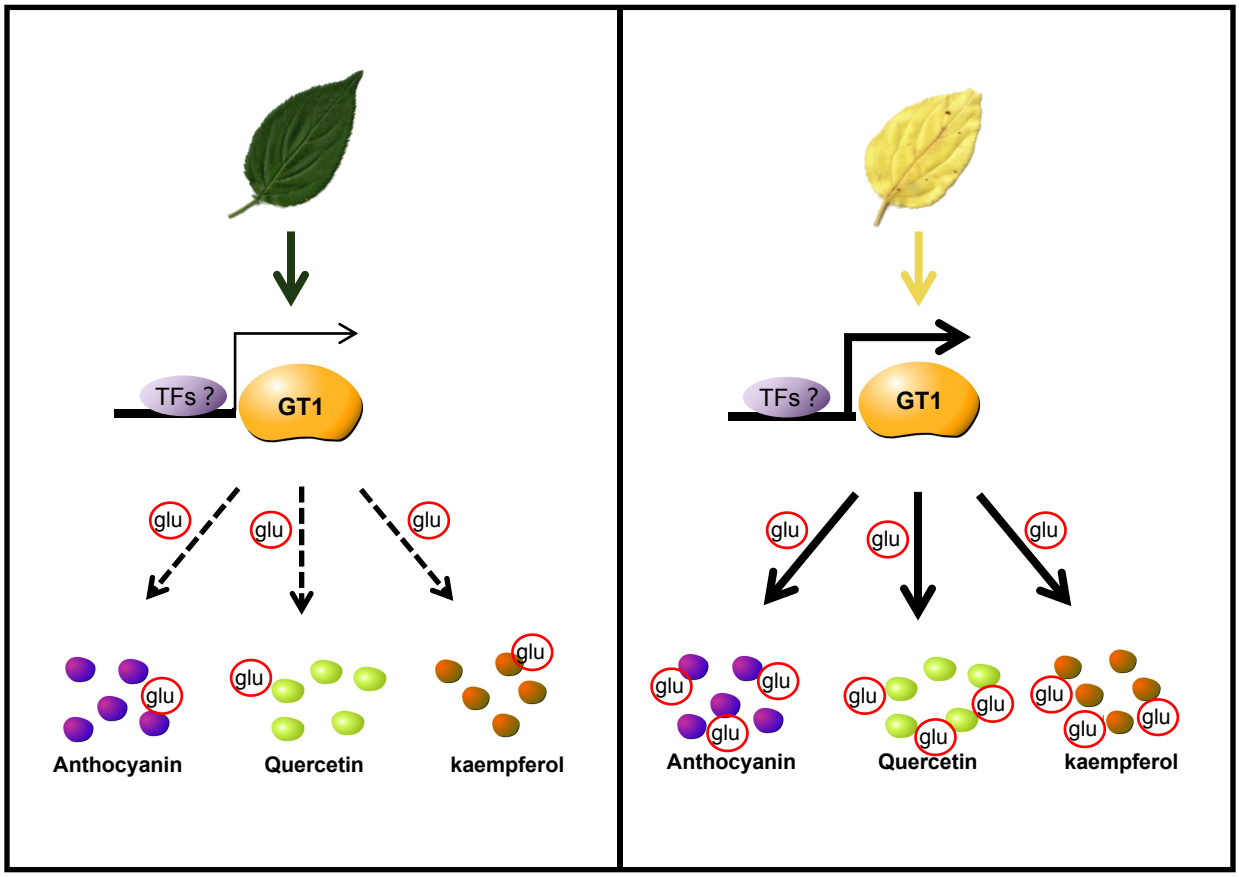
TFs ?
GT1
glu
glu
glu
glu
glu
glu
Anthocyanin
Quercetin
kaempferol
TFs ?
GT1
glu
glu
glu
glu
glu
glu
glu
glu
glu
glu
glu
glu
Anthocyanin
Quercetin
kaempferol

FigureS1

(a)

PFPAQGHIIPMLELAKLLVSR
GFHITFVNTEFNHKRLLNSLG
ALDVAEEFGIPRVLFFTSSAA
GLTPLKDESYLTNGYLDTVIDWIPGMKDIRLRDLPTFIRTTBPNDIMFNF
GIIVNTFYELEPAALDALSSI
CLEWLDSQPPNSVVYVCFGSITVFTPEQLKELAWGLENSGQPFLWVVRPD
VLPEGFLERTKDRGLVV
QVEVLNHPSVGGFLTHCGWNSTLESLSAGVPMJCWPLFAEQ
VKRDEVEKLVRELMEGEEGKEMRKK
KEKAKEALEEGGSSYKNLDNL

(b)

name	Chromosomelocation	pI/Mw	No.ofAA	SubCellularLoc.
MD00G1052900	0	5.71/54302.57	484	Cellmembrane;Chloroplast
MD00G1055100	0	6.59/55174.02	494	Cellmembrane;Chloroplast
MD01G1148700	1	4.93/50931.24	458	Cellmembrane
MD01G1210700	1	6.42/52922.21	487	Chloroplast
MD02G1153200	2	5.52/53955.33	487	Cellmembrane;Chloroplast
MD06G1103400	6	6.26/53584.82	489	Chloroplast
MD06G1103500	6	6.01/28132.51	254	Chloroplast
MD06G1103600	6	9.01/42656.50	384	Cellmembrane;Chloroplast;Nucleus
MD06G1200500	6	6.09/51979.83	470	Chloroplast
MD07G1007600	7	5.96/53462.68	479	Cellmembrane
MD07G1208800	7	5.67/52078.79	466	Cellmembrane
MD08G1185000	8	5.33/52677.42	474	Cellmembrane;Chloroplast
MD08G1185500	8	5.13/53964.07	484	Cellmembrane;Chloroplast
MD08G1185700	8	5.51/54059.32	485	Cellmembrane
MD08G1219100	8	5.66/53380.56	482	Cellmembrane
MD09G1064700	9	5.63/52810.73	472	Cellmembrane
MD09G1064900	9	5.20/50713.39	457	Cellmembrane
MD09G1065400	9	5.45/50288.70	454	Cellmembrane;Chloroplast
MD09G1136200	9	5.59/54088.95	487	Cellmembrane
MD09G1141500	9	5.32/52228.74	473	Cellmembrane
MD09G1141700	9	5.45/52986.65	484	Cellmembrane
MD09G1143400	9	5.80/40028.91	360	Chloroplast
MD15G1357700	15	5.37/51503.12	457	Cellmembrane;Chloroplast.
MD15G1407300	15	5.38/53150.90	481	Chloroplast
MD17G1058100	17	5.21/50917.28	456	Cellmembrane
MD17G1058200	17	5.10/50505.78	454	Cellmembrane
MD17G1100000	17	6.54/53434.15	482	Cellmembrane
MD17G1124900	17	5.44/53689.87	479	Chloroplast
MD17G1125900	17	5.61/53482.31	477	Cellmembrane
MD17G1126300	17	5.78/54539.95	486	Cellmembrane;Chloroplast
MD17G1126400	17	4.62/21711.83	196	Chloroplast
MD17G1126900	17	5.23/35425.56	314	Chloroplast;Peroxisome
MD17G1129500	17	5.16/52397.21	475	Cellmembrane

FigureS2

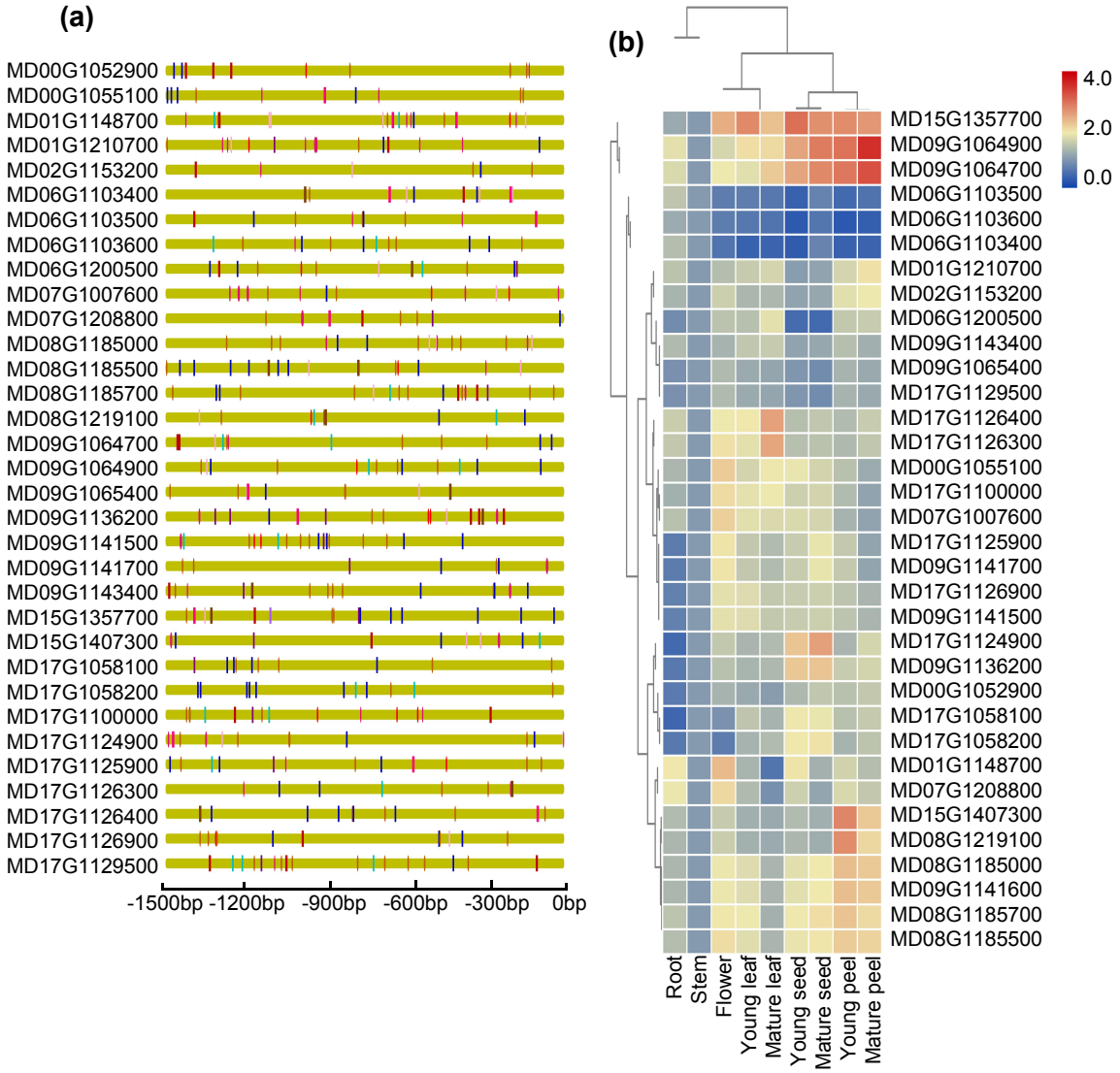
(a)
MD00G1052900
MD00G1055100
MD01G1148700
MD01G1210700
MD02G1153200
MD06G1103400
MD06G1103500
MD06G1103600
MD06G1200500
MD07G1007600
MD07G1208800
MD08G1185000
MD08G1185500
MD08G1185700
MD08G1219100
MD09G1064700
MD09G1064900
MD09G1065400
MD09G1136200
MD09G1141500
MD09G1141700
MD09G1143400
MD15G1357700
MD15G1407300
MD17G1058100
MD17G1058200
MD17G1100000
MD17G1124900
MD17G1125900
MD17G1126300
MD17G1126400
MD17G1126900
MD17G1129500
-1500bp -1200bp -900bp -600bp -300bp 0bp
(b)
4.0
2.0
0.0
MD15G1357700
MD09G1064900
MD09G1064700
MD06G1103500
MD06G1103600
MD06G1103400
MD01G1210700
MD02G1153200
MD06G1200500
MD09G1143400
MD09G1065400
MD17G1129500
MD17G1126400
MD17G1126300
MD00G1055100
MD17G1100000
MD07G1007600
MD17G1125900
MD09G1141700
MD17G1126900
MD09G1141500
MD17G1124900
MD09G1136200
MD00G1052900
MD17G1058100
MD17G1058200
MD01G1148700
MD07G1208800
MD15G1407300
MD08G1219100
MD08G1185000
MD09G1141600
MD08G1185700
MD08G1185500
Root
Stem
Flower
Young leaf
Mature leaf
Young seed
Mature seed
Young peel
Mature peel

FigureS3

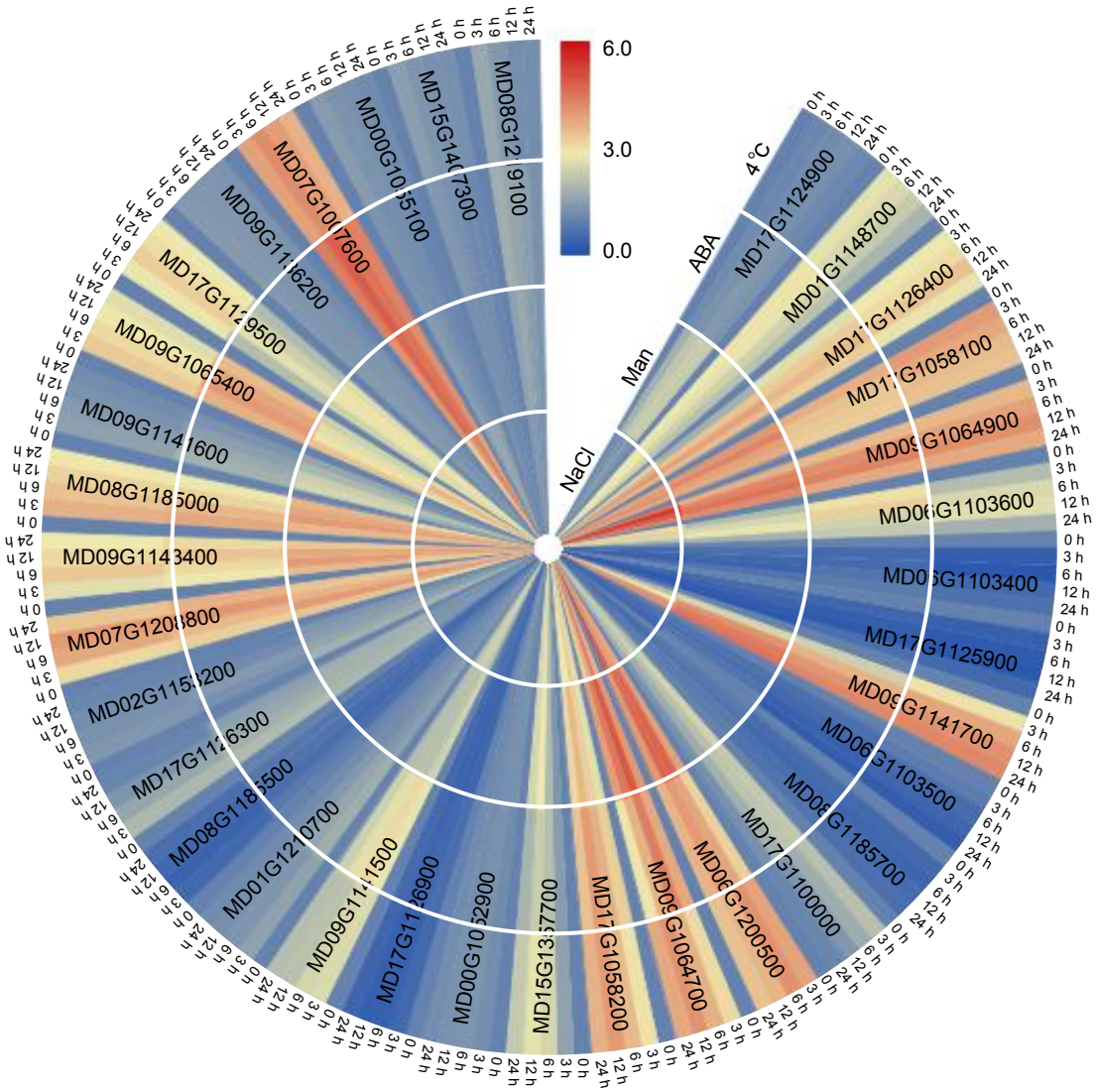
6.0
3.0
0.0
4 °C
ABA
Man
NaCl
MD08G1219100
MD15G1407300
MD00G1015100
MD07G1007600
MD09G1116200
MD17G1129500
MD09G1065400
MD09G1141600
MD08G1185000
MD09G1143400
MD07G1208800
MD02G1155200
MD17G1116300
MD08G1185500
MD01G1210700
MD09G1141500
MD17G1126900
MD00G1052900
MD15G1357700
MD17G1058200
MD09G1064700
MD06G1200500
MD17G1100000
MD08G1185700
MD06G1103500
MD09G1141700
MD17G1125900
MD06G1103400
MD06G1103600
MD09G1064900
MD17G1058100
MD17G1126400
MD01G1148700
MD17G1124900
0 h
3 h
6 h
12 h
24 h

FigureS4

Name	Substrates	Specificactivity(nkat/mgprotein)	Structures
MdGT1	Anthocyanin	3.47±0.16	C15H11O6+
	Quercetin	1.25±0.11	C15H10O7
	Kaempferol	1.08±0.07	C15H10O6
	Procyanidin	ND	
	Naringenin	ND	
	Ferulicacid	ND	
	Caffeicacid	ND	
	Cinnamicacid	ND	
	Sinapicacid	ND	
	Sinainicaldehyde	ND	
	Coniferol	ND	

FigureS5

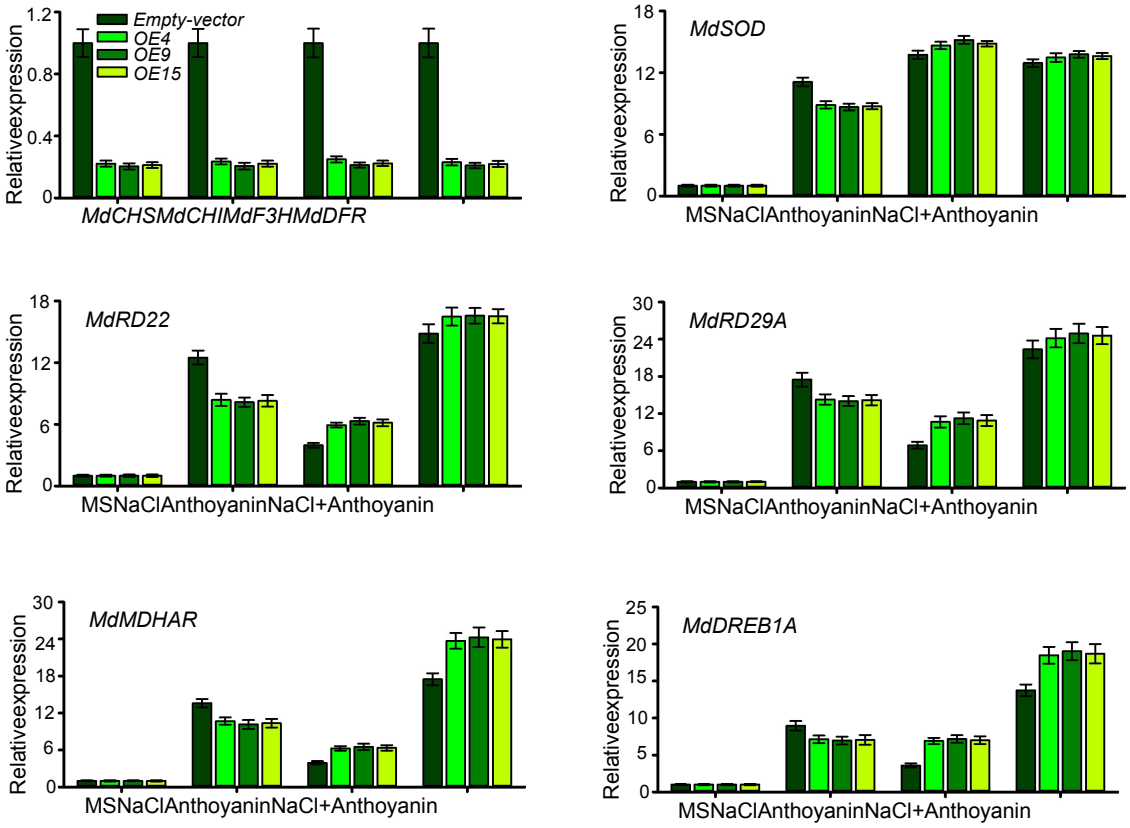
Empty-vector
OE4
OE9
OE15
Relativeexpression
MdCHS
MdCHI
MdF3H
MdDFR
MdSOD
MdRD22
MdRD29A
MdMDHAR
MdDREB1A
MS
NaCl
Anthoyanin
NaCl+Anthoyanin

FigureS6

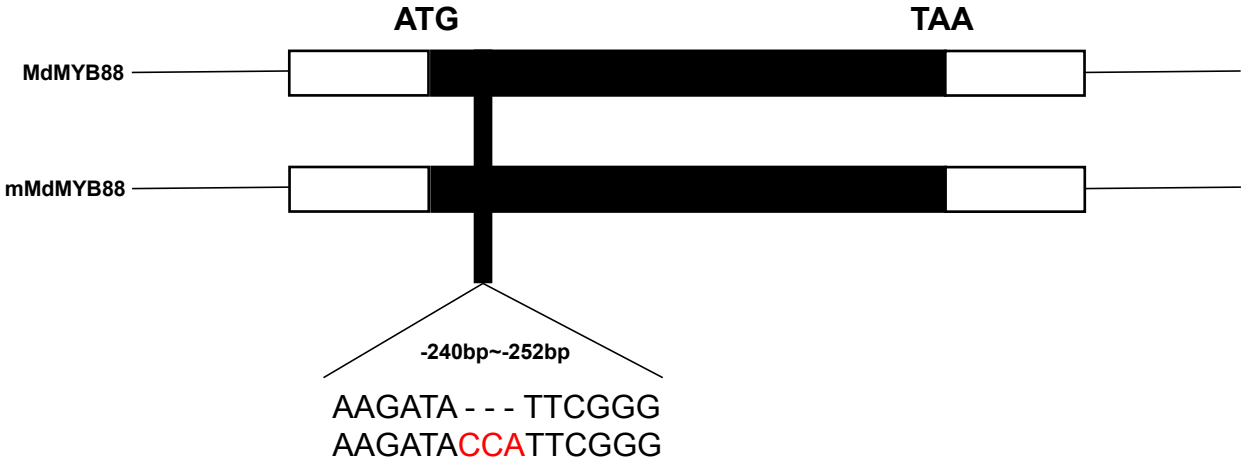
ATG
TAA
MdMYB88
mMdMYB88
-240bp~-252bp
AAGATA - - - TTCGGG
AAGATACCATTCGGG